Supplementary Information

Yellow and Red Polymorphic Co-crystals of Phenyl-Substituted Pyrazinacene and Naphthalene via π-Hole···π Interactions

K. Nakada, G. J. Richards, A. Hori*

*Corresponding author (e-mail: ahori@shibaura-it.ac.jp)

Table of Contents

S1. Preparation and TG studies of 1 with napthalene (2)

*S1-1 Preparation of **1•2** (**Y** and **R**)*

A chloroform solution (6 mL) of **1** (3.0 mg, 9.0 μmol) and **2** (11 mg, 90 μmol) was prepared in a vial. The solvent was allowed to evaporate naturally over one day, resulting in the precipitation of the yellow co-crystal of **1•2** (**Y**) along with transparent crystals of **2**. Using the same method, a chloroform solution of **1** (3.0 mg, 9.0 μmol) and **2** (1.1 mg, 9.0 μmol) was evaporated, yielding the red co-crystal of **1•2** (**R**).

When slow evaporation of chloroform with isopropanol was performed in a test tube, both **1•2** (**Y** and **R**) formed larger crystals. However, no selective formation was observed due to the volatilization of naphthalene.

S1-2. Thermogravimetric (TG) results

TG results indicate that the guest release process is consistent with 1:1 cocrystal for a) **1•2** (**Y**) and b) **1•2** (**R**), as shown in **Figure S1**. For both crystals, it was found that the removal process proceeds in two steps.

For **1·2** (**Y**), during the first step, heating up to around 90 °C resulted in the release of excess naphthalene adhered to the surface of the powder. A second-step reduction was observed between 90 °C and 105 °C. The measured mass loss at 105 °C was 27.9%, which is close to the calculated value of 27.7%.

For **1·2** (**R**), during the first step, naphthalene adhered to the surface of the powder was released up to around 70 °C. A second-step reduction was observed between 70 °C and 90 °C. The measured mass loss at 90 °C was 23.7%, which is close to the calculated value of 27.7%.

Because napthalene (**2**) can easily evaporate from the crystals at room temperature, it was not possible to easily distinguish napthalene (**2**) on the surface of the crystals from napthalene inside the crystals.

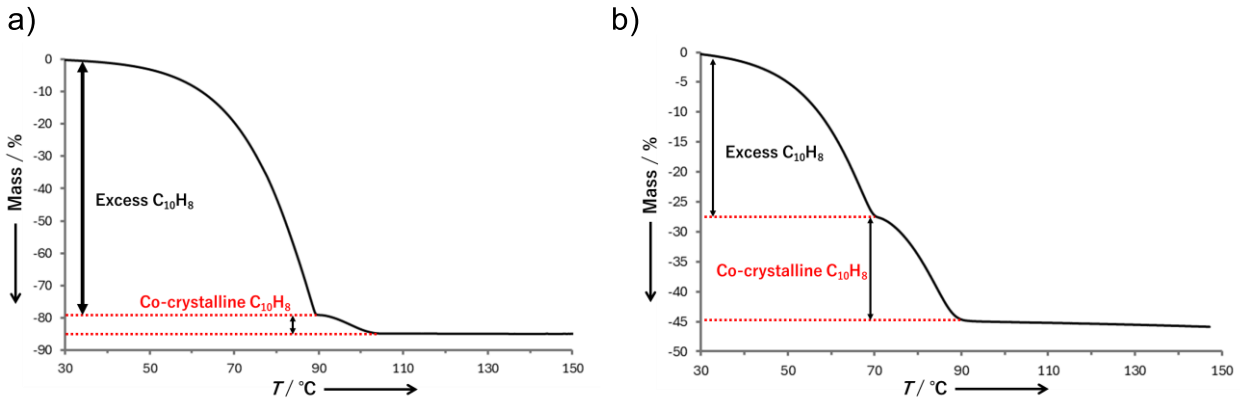

Figure S1. TG of a) **1•2** (**Y**) and b) **1•2** (**R**). The scan rate was 5.0 °C min^{-1}.

S2. Crystal data and Hirshfeld surface analysis of 1•2

*S2-1. Crystal data of **1•2 (Y)** and **1•2 (R)***

The crystal data of two structures are shown in **Table S1**, and each structure was shown in **Figures S2-3**.

Table S1. Crystal data and structure refinements for **1•2** (**Y**) and **1•2** (**R**)

	1•2 (**Y**)	**1•2** (**R**)
Chemical formula	$C_{20}H_{10}N_6$•$C_{10}H_8$	$C_{20}H_{10}N_6$•$C_{10}H_8$
Description, color	Prismatic, yellow	Plate, red
Crystal size	0.33 × 0.25 × 0.07	0.28 × 0.21 × 0.16
Formula weight	462.50	462.50
T [K]	160	160
Crystal system	Monoclinic	Monoclinic
Space group	$P2_1/c$	$P2_1/c$
a [Å]	14.0115 (15)	12.312 (6)
b [Å]	7.1139 (7)	7.042 (4)
c [Å]	24.401 (3)	26.902 (13)
α [°]	90	90
β [°]	102.624 (4)	98.740 (17)
γ [°]	90	90
V [Å^3]	2373.4 (4)	2306 (2)
Z	4	4
D_c [g cm^{-3}]	1.294	1.332
F(000)	960	960
R_{int}	0.063	0.072

Reflections measured	25961	22427
Reflections independent	4199	4065
GOF	1.041	1.076
$R\,[(I) > 2\sigma(I)]$	0.048	0.065
$wR\,(F_o^2)$	0.128	0.149
CCDC No.	2419629	2419630

*S2-2. X-ray crystal structure of **1•2 (Y)***

In the crystal structure (**Figure S2**), whole structures of **1** and napthalene (**2**) were observed in the asymmetric unit. H atoms attached to C atoms were refined as riding on their idealized positions, with C-H = 0.95 Å for aromatic atoms.

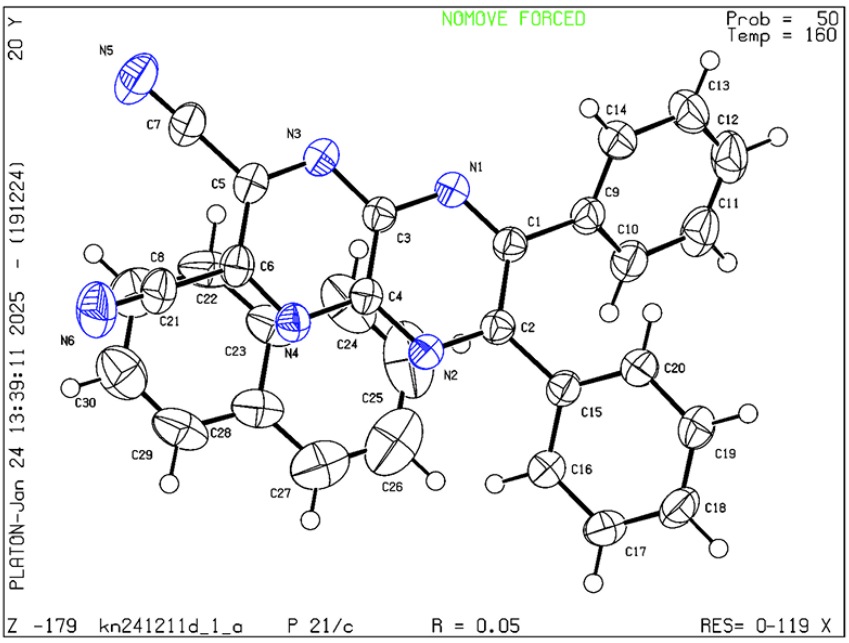

Figure S2. The molecular structure of **1•2** (**Y**) drawing by PLATON from checkCIF.

*S2-3. X-ray crystal structure of **1•2 (R)***

In the crystal structure (**Figure S3**), whole structures of **1** and napthalene (**2**) were observed in the asymmetric unit. H atoms attached to C atoms were refined as riding on their idealized positions, with C-H = 0.95 Å for aromatic atoms.

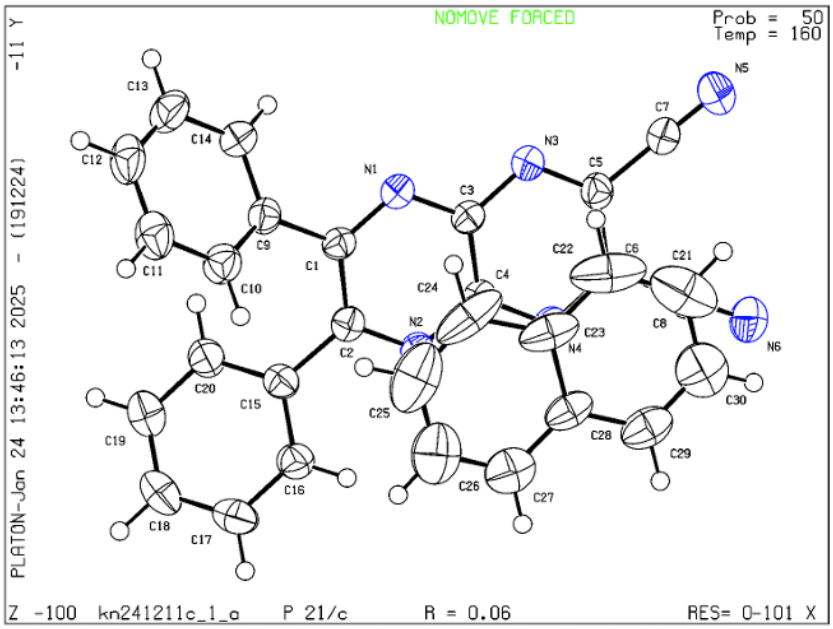

Figure S3. The molecular structure of **1•2** (**R**) drawing by PLATON from checkCIF.

*S2-4. Fingerprint plots of **1** in **1•2** (**Y**)*

HS analysis shows the contribution of intermolecular interactions of **1•2** (**Y**) (**Figure S4**).

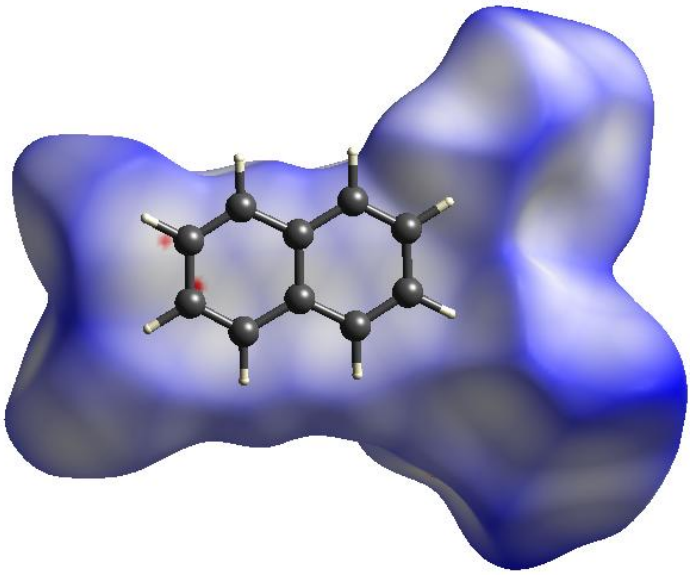

C (in)···All (out) 24.3% C (in)···C (out) 6.7% C (in)···N (out) 2.8% C (in)···H (out) 14.9%

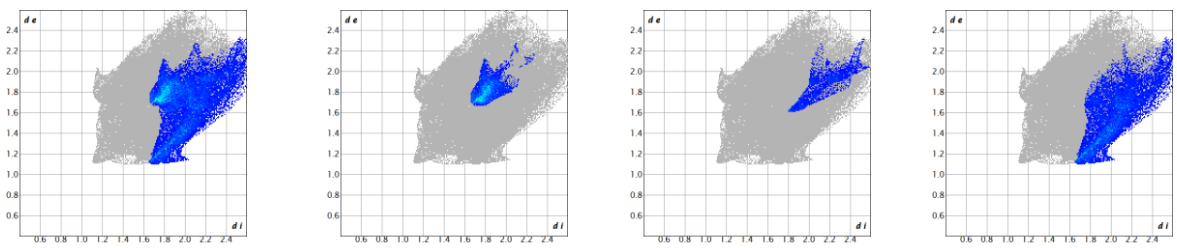

N (in)···All (out) 29.4% N (in)···C (out) 5.5% N (in)···N (out) 0.7% N (in)···H (out) 23.2%

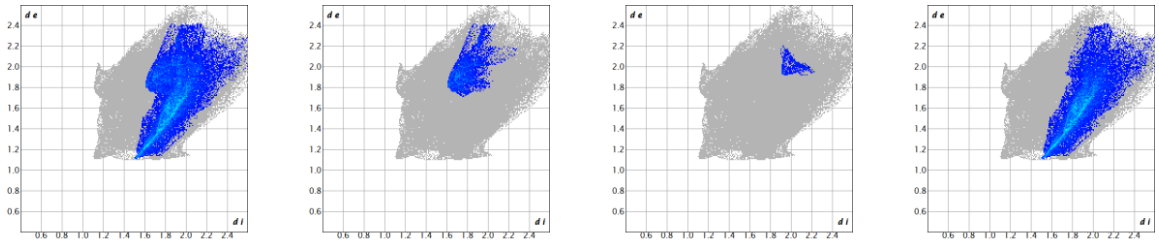

H (in)···All (out) 46.2% H (in)···C (out) 5.7% H (in)···N (out) 6.7% H (in)···H (out) 33.9%

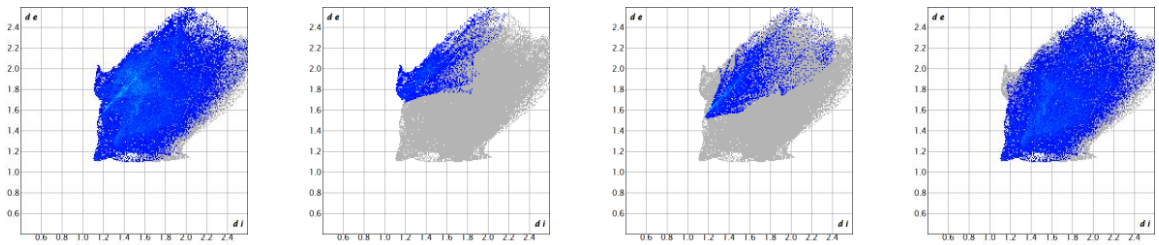

Figure S4. Fingerprint plots for **1** in **1•2** (**Y**) showing d_e and d_i of 0.4–2.6 Å for all atoms.

*S2-5. Fingerprint plots of **2** in **1•2** (**Y**)*

HS analysis shows the contribution of intermolecular interactions of **1•2** (**Y**) (**Figure S5**).

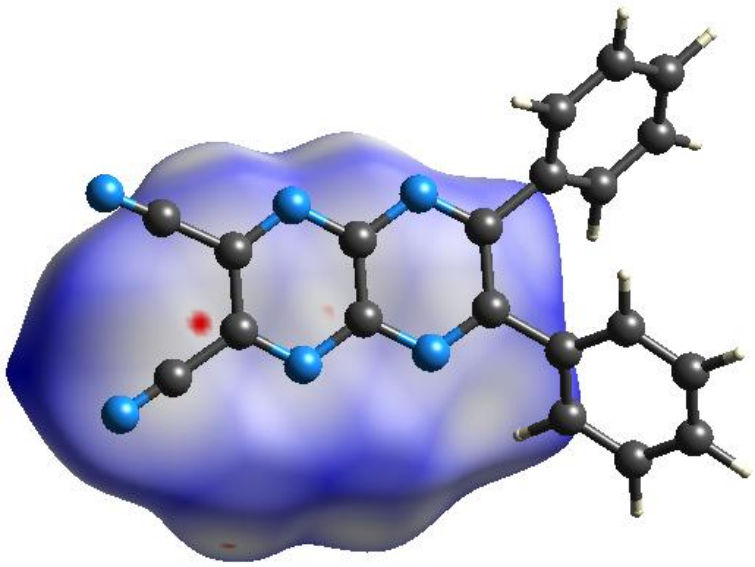

C (in)···All (out) 26.4% C (in)···C (out) 7.0% C (in)···N (out) 5.6% C (in)···H (out) 13.8%

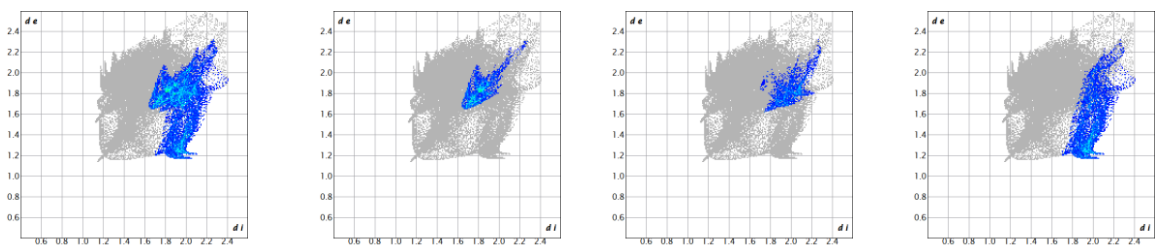

H (in)···All (out) 73.6% H (in)···C (out) 21.5% H (in)···N (out) 21.6% H (in)···H (out) 30.5%

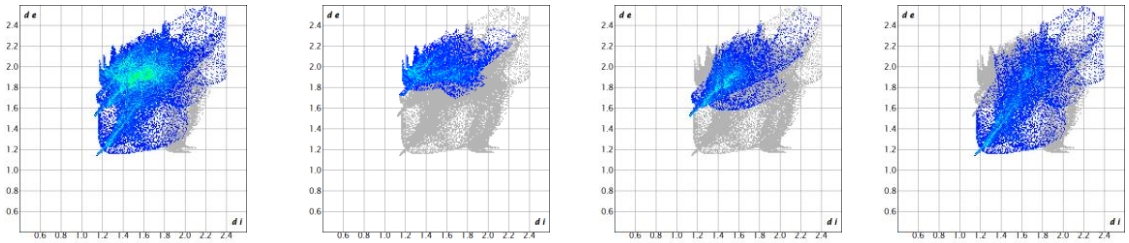

Figure S5. Fingerprint plots for **2** in **1•2** (**Y**) showing d_e and d_i of 0.4–2.6 Å for all atoms.

*S2-6. Fingerprint plots of **1** in **1•2 (R)***

HS analysis shows the contribution of intermolecular interactions of **1•2** (**R**) (**Figure S6**).

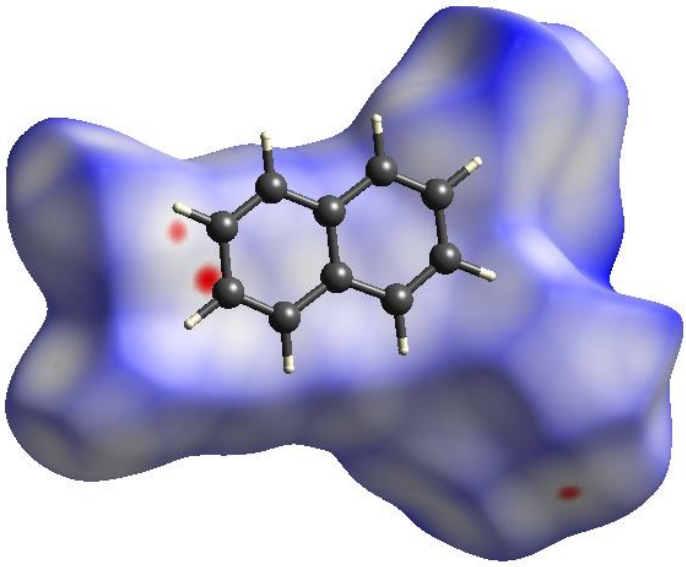

C (in)···All (out) 25.0% C (in)···C (out) 5.9% C (in)···N (out) 4.7% C (in)···H (out) 14.5%

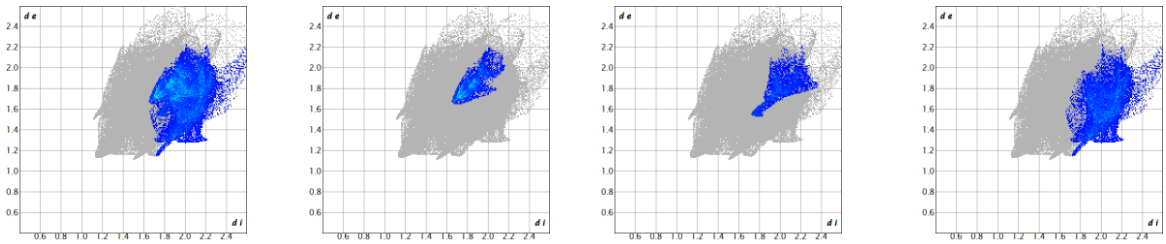

N (in)···All (out) 29.5% N (in)···C (out) 6.4% N (in)···N (out) 1.1% N (in)···H (out) 22.0%

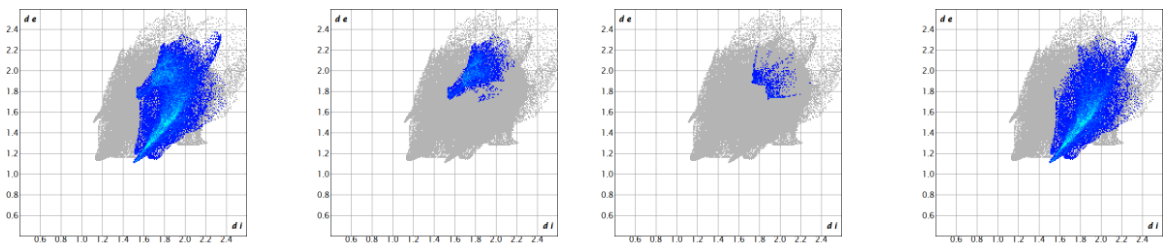

H (in)···All (out) 45.5% H (in)···C (out) 5.2% H (in)···N (out) 6.7% H (in)···H (out) 33.6%

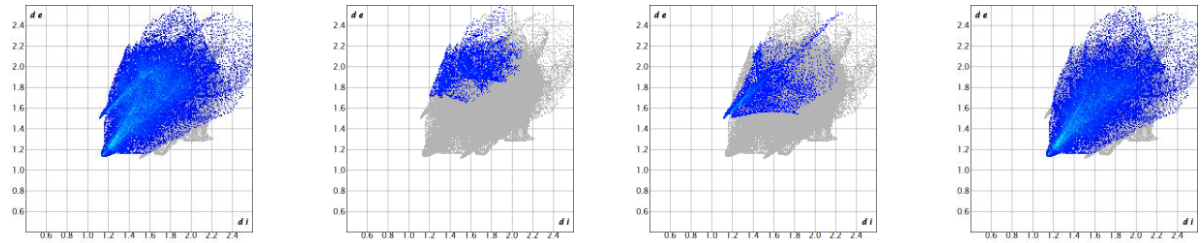

Figure S6. Fingerprint plots for **1** in **1•2** (**R**) showing d_e and d_i of 0.4–2.6 Å for all atoms.

*S2-7. Fingerprint plots of **2** in **1•2 (R)***

HS analysis shows the contribution of intermolecular interactions of **1•2** (**R**) (**Figure S7**).

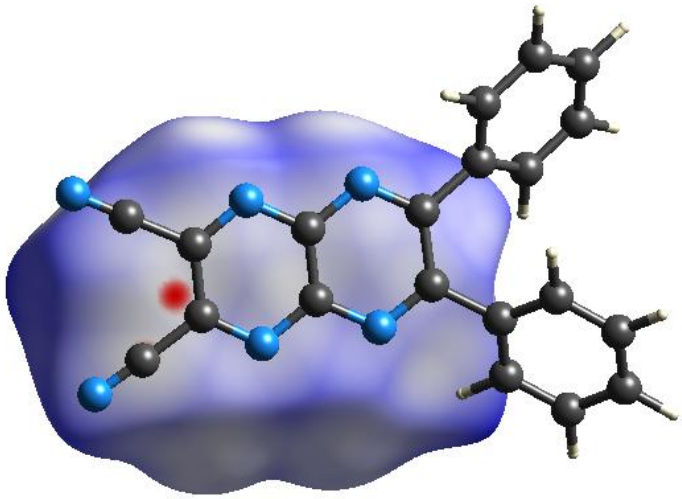

C (in)···All (out) 25.5% C (in)···C (out) 14.2% C (in)···N (out) 8.3% C (in)···H (out) 3.1%

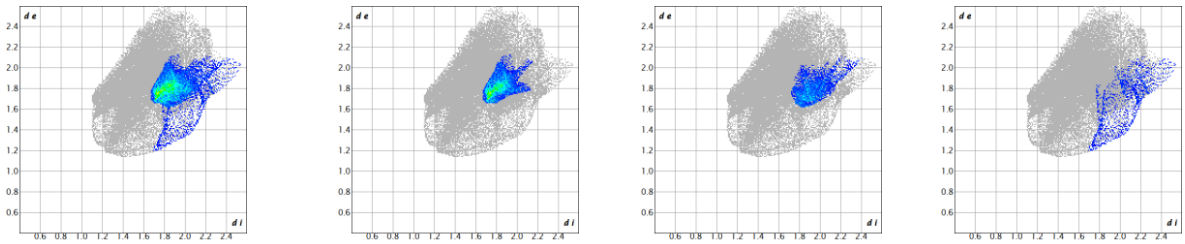

H (in)···All (out) 74.5% H (in)···C (out) 14.4% H (in)···N (out) 24.0% H (in)···H (out) 36.1%

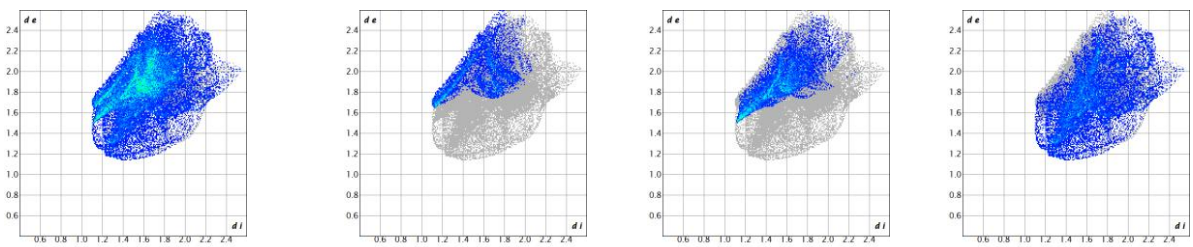

Figure S7. Fingerprint plots for **2** in **1•2** (**R**) showing d_e and d_i of 0.4–2.6 Å for all atoms.

S3. pXRD studies of 1 with napthalene (2)

S3-1. pXRD studies

Powder X-ray diffraction (pXRD) pattern shows that the obtained powder matches the sum of the peaks calculated from the co-crystal and those of pure naphthalene (**Figure S8-9**).

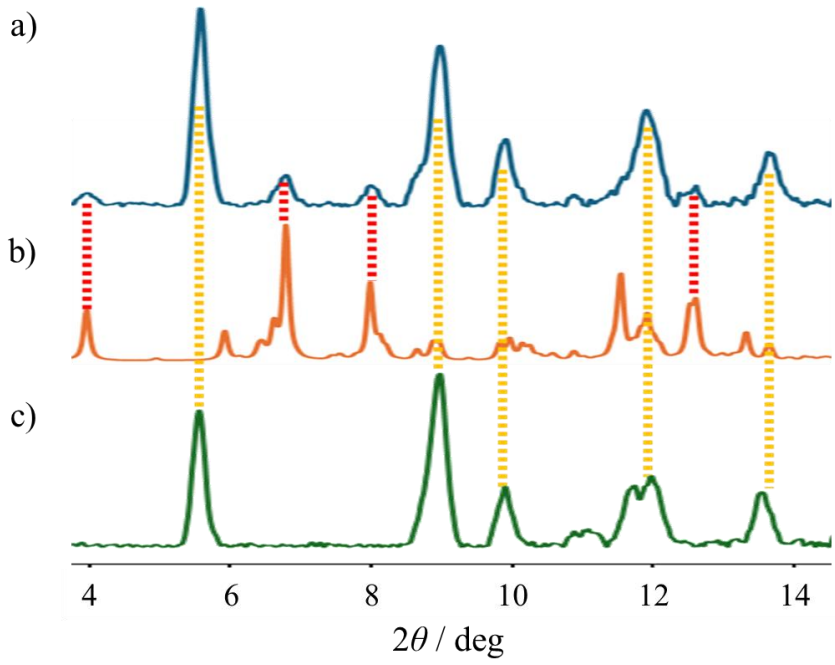

Figure S8. pXRD patterns: a) powder sample of **1•2** (**Y**), b) simulation from the single crystal of **1•2** (**Y**) and c) powder sample of **2**.

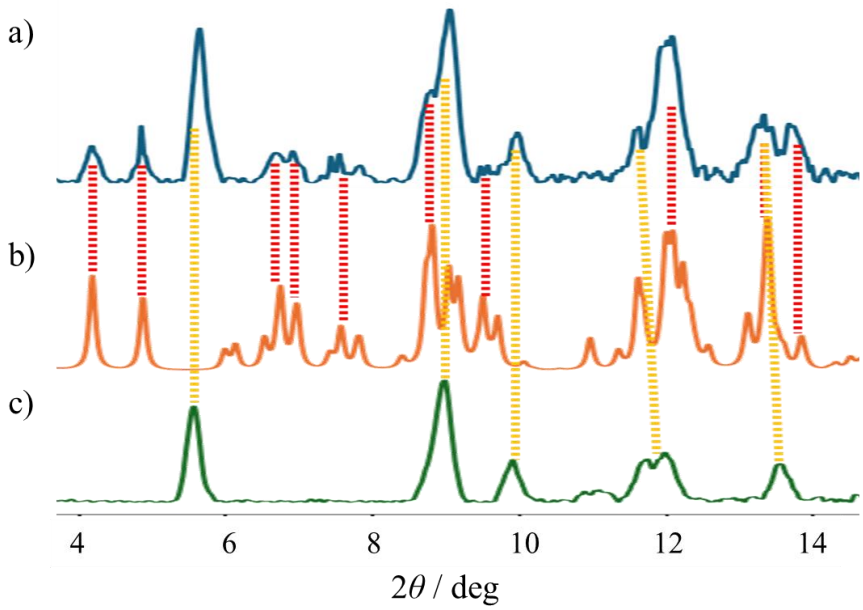

Figure S9. pXRD patterns: a) powder sample of **1•2** (**R**), b) simulation from the single crystal of **1•2** (**R**) and c) powder sample of **2**.

S4. DFT calculations of co-crystal 1•2

Electrostatic potential (ESP) maps and molecular orbital energies were calculated for the crystal structure, which consists of two molecules of **1** and two molecules of naphthalene (**2**), using DFT with B3LYP 6-311+G (2df, 2p) sets, which clearly support the spectroscopic studies (**Figure S10-11**). The calculation results were in qualitatively good agreement with the spectroscopic results of **Figure 5b** and **Figure 5c**.

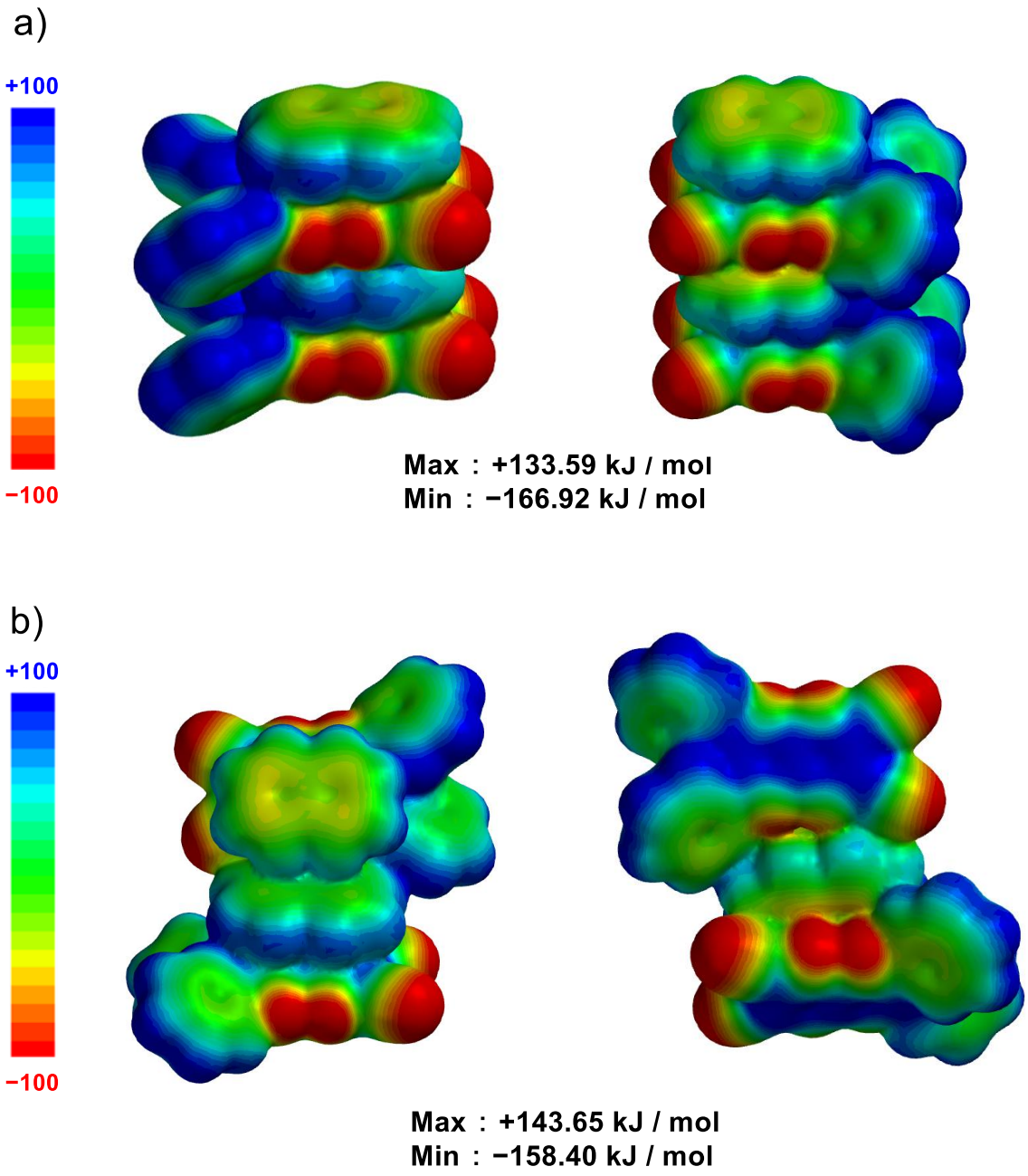

Figure S10. The energy potential maps of front and back views of a) **1•2** (**Y**) and b) **1•2** (**R**) from the crystal structures: the color of the potential is shown between −100 kJ mol^{-1} (red) to +100 kJ mol^{-1} (blue).

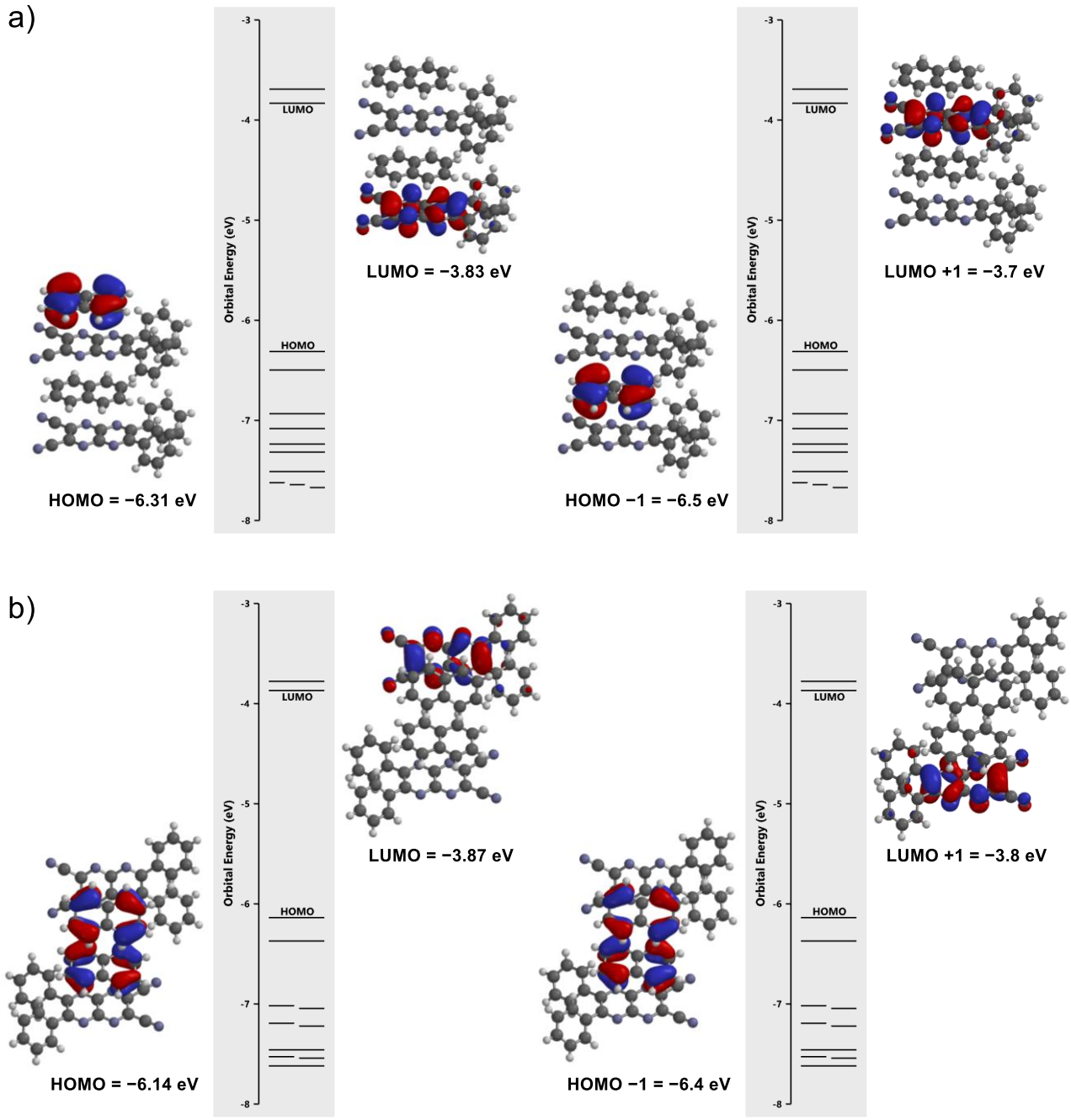

Figure S11. Molecular orbital energy level diagrams of a) **1•2** (**Y**) and b) **1•2** (**R**).

Predicted UV/vis absorption spectra of **1** and the model structures of **1•2** (**Y**) and **1•2** (**R**) were obtained using TDDFT with the cam-B3LYP/6-311G** method, based on the crystal structure containing two molecules of **1** and two molecules of naphthalene (**2**). The broad peaks, attributed to charge-transfer absorption bands, were observed experimentally for both **1•2** (**Y**) and **1•2** (**R**). These peaks were also confirmed by spectra predicted based on their structures. Although the predicted spectra are blue shifted compared to the experimental data, the absorption band of **1•2** (**R**) appears at a longer wavelength than that of **1•2** (**Y**), which is consistent with the experimental results (**Figure S12**).

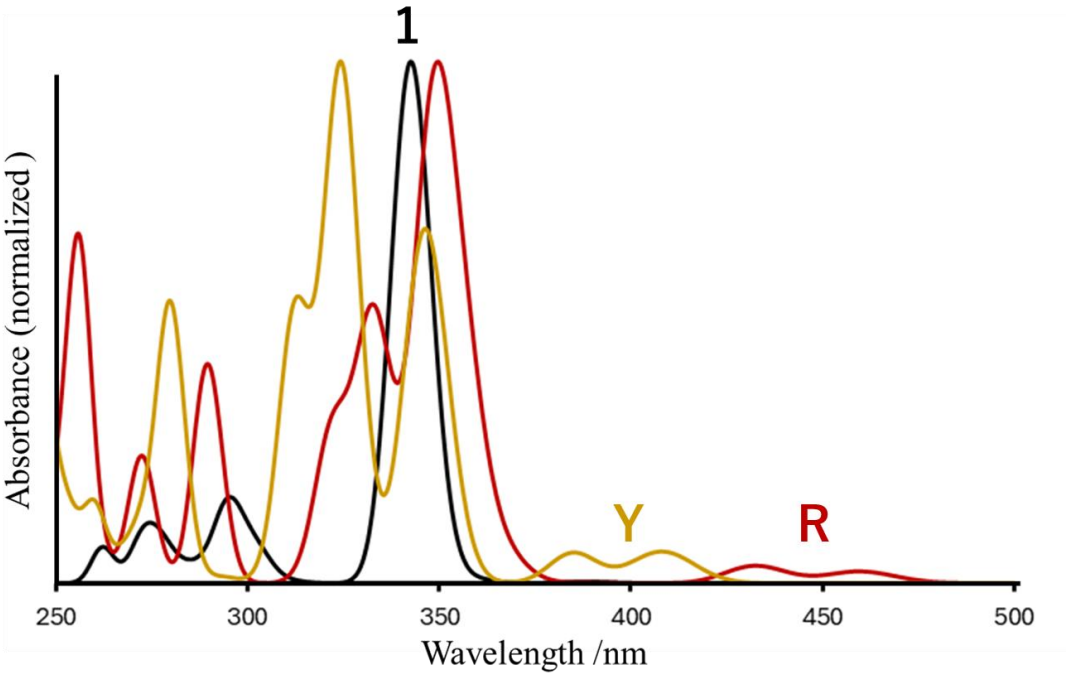

Figure S12. Predicted UV/vis absorption spectra of **1**, **1•2** (**Y**) and **1•2** (**R**) calculated using TDDFT cam-B3LYP 6-311G** method.